Zoogeochemical impacts of freshwater mussels on stream metabolism are mediated by their ecophysiological and behavioral traits

Jonathan W. Lopez[1,2], Matthew B. Lodato[1,3], Carla L. Atkinson[1,4]

[1]Department of Biological Sciences, University of Alabama, Tuscaloosa, Alabama USA

E-mail addresses: [2]jwlopez@ua.edu; [3]mlodato@crimson.ua.edu; [4]carla.l.atkinson@ua.edu

Received 22 April 2024; Accepted 22 October 2024; Published online XX Month 20XX;

Associate Editor, Brian Helms.

Freshwater Science, volume 44, number 1, March 2025. Published by The University of Chicago Press for the Society for Freshwater Science. https://doi.org/10.1086/XXXXXX

Abstract: Animals can have strong impacts on biogeochemical processes. These zoogeochemical impacts occur via biomass-dependent direct effects and via indirect effects that are linked to the ecophysiological and behavioral traits of animals. In streams, animals may affect C transport and mineralization by altering ecosystem metabolism—the balance of ecosystem respiration (ER) and gross primary productivity (GPP). Freshwater mussels occur in dense aggregations and can affect stream ecosystem metabolism, but these effects depend on interspecific variation in traits. Our goal was to test how the impacts of mussel aggregations on ecosystem metabolism are mediated by species traits. We conducted a field experiment using custom self-contained chambers designed to measure ecosystem metabolic rates. Each chamber contained 1 of 4 monospecific mussel treatments with contrasting traits. We quantified ER and GPP in each chamber during late-summer and autumn incubations. We also tracked individual mussel movement patterns during the late-summer incubations to test for bioturbation effects. ER increased with mussel biomass and thermal sensitivity, and GPP increased with N excretion. Increases in ER in the presence of thermally sensitive mussels were larger in the late summer. Mussel vertical movement frequency and depth varied by species, but horizontal movement did not. Burial depth and vertical movement frequency were higher in thermally sensitive species than tolerant species, suggesting sensitive species respond both behaviorally and physiologically to temperature. Increased movement frequency appeared to increase background ER via bioturbation. Comparison of benthic CO_2 exchange between mussel species treatments suggested that mussels drive detectable changes in stream C cycles. Overall, our findings indicate that mussel ecophysiological and behavioral traits constrain their impacts on ecosystem metabolism. An improved understanding of how traits mediate zoogeochemical effects may improve our ability to anticipate and predict changes in freshwater C cycling and create an interdisciplinary

synergy between biogeochemistry and conservation.

Key words: respiration, primary productivity, carbon, biomass, excretion, nutrient diffusing substrate, burrowing, bioturbation, movement, unionid

INTRODUCTION

Animals can have strong impacts on biogeochemical processes, such as C cycling (Dirzo et al. 2014, Schmitz et al. 2014, 2018). These zoogeochemical effects (sensu Schmitz et al. 2018) can be large relative to the proportion of animal biomass in the ecosystem because animals not only have biomass-dependent direct effects but also indirect effects that propagate through the community (Schmitz et al. 2014, Schmitz and Leroux 2020). Zoogeochemical effects on the C cycle are best understood in terrestrial and coastal marine ecosystems (McInnes et al. 1992, Wilmers et al. 2012, Strickland et al. 2013, Atwood et al. 2018), but animals also influence freshwater C pools and fluxes via ecosystem engineering, trophic interactions, and the creation of biogeochemical hotspots (Schindler et al. 1997, Hall et al. 2003, Atwood et al. 2013, Atkinson et al. 2018, Nummi et al. 2018). However, freshwater animals are subject to disproportionate rates of defaunation compared with terrestrial and marine animals, which may alter freshwater zoogeochemical impacts on the C cycle (Strayer and Dudgeon 2010, Reid et al. 2019). Furthermore, freshwater ecosystems are critical components of the global C cycle (Cole et al. 2007, Raymond et al. 2013, Hotchkiss et al. 2015, Maranger et al. 2018). Thus, an improved understanding of zoogeochemical effects on freshwater C cycles should also yield improved predictions of changes in C storage and exchange.

C transport and mineralization in streams is governed by ecosystem metabolism, or the balance of ecosystem respiration (ER) and gross primary productivity (GPP; Hall et al. 2016). The proximate drivers of stream metabolism are typically photosynthetically active radiation (PAR), temperature, and nutrient availability (Mulholland et al. 2001, Munn et al. 2023). However, animals may also alter ER and GPP—and thereby C cycling—through direct and indirect mechanisms that are tied to their ecophysiological and behavioral traits, including

metabolic rates, trophic compartments, and movement activities (Steinberg and Landry 2017, Schmitz and Leroux 2020). The trait that most directly regulates zoogeochemical effects on stream metabolism is organismal respiration rate because ER is the sum of organismal respiration across the ecosystem. However, these impacts may be small or variable, with estimates of the direct contributions of animals to whole-stream ER as low as 1% for fishes (Hall 1972) and ranging broadly from 2 to 25% for macroinvertebrates, depending on habitat type (Wilhm 1970). On the other hand, indirect zoogeochemical effects can be quite large. For example, trophic cascades resulting from the addition of a stonefly predator to experimental streams caused a 94% reduction in CO_2 efflux (Atwood et al. 2013). In an Andean piedmont stream, experimental removal of detritivorous fish indirectly led to a 150% decrease in the ratio of GPP to ER (Taylor et al. 2006). Collectively, these studies indicate the potentially significant role that animals play in constraining freshwater C cycles.

Freshwater mussels (Unionida) are burrowing bivalves that can have strong zoogeochemical effects in streams because they aggregate in dense, species-rich assemblages (Atkinson and Vaughn 2015, Atkinson et al. 2018, Hopper et al. 2021, Atkinson and Forshay 2022). Within an aggregation, species express broad variation in ecophysiological traits, such as body size, metabolic rates, and thermal tolerance (Spooner and Vaughn 2008, Vaughn 2012, van Ee et al. 2022). Such traits mediate the strength of mussel zoogeochemical effects. For example, mussel respiration can directly contribute 16 to 43% of ER at summer base flow (Atkinson et al. 2018), and mussels can alter GPP via excretion of N and P, which fertilizes primary producers (Allen et al. 2012, Atkinson et al. 2013, Lopez et al. 2020). Mussel respiration and excretion rates increase with temperature because mussels are ectotherms. Mussel species can be classified into 1 of 2 thermal tolerance guilds depending on the relative changes they experience in their

respiration and excretion rates at elevated temperatures. The thermally sensitive guild includes mussels that tend to catabolize resources from their own tissue at high temperatures, whereas the thermally tolerant guild can continue to assimilate resources via anabolism (Spooner and Vaughn 2008). Temperature-related increases in excretion and respiration rates are often higher in thermally sensitive species than thermally tolerant species (Spooner and Vaughn 2008, van Ee et al. 2022).

Additionally, mussel species vary in their behavioral traits, such as the distance and frequency with which they burrow through the substrate (Allen and Vaughn 2009, Gough et al. 2012, Newton et al. 2015, Curley et al. 2022). Mussel burrowing may have indirect effects on benthic stream metabolism via bioturbation. Bioturbation-driven alterations to benthic metabolism tend to increase ER and CO_2 efflux from the sediment by increasing O_2 penetration and, thereby, aerobic respiration, but the strength of bioturbation depends on animals' specific burrowing traits (Mermillod-Blondin and Rosenberg 2006, Thomson et al. 2019). The rate and depth at which mussels burrow are functions of species identity and environmental conditions like temperature and water depth (Allen and Vaughn 2009, Newton et al. 2015, Curley et al. 2022). For example, horizontal movement allows thermally sensitive species to track receding water levels, whereas more-tolerant species may simply burrow deeper in the sediment to escape emersion and high temperatures (Gough et al. 2012). Although mussel bioturbation effects have been studied (Matisoff et al. 1985), the potential for mussel behavioral traits to mediate their impacts on benthic metabolism has yet to be tested.

In this study we sought to understand how mussel species identity and traits mediate their influence on benthic metabolism. We sought to answer the overall question of which mussel species traits are most important in mediating benthic metabolism in mussel beds. We tested the

following hypotheses: H1) after accounting for environmental drivers (e.g., PAR, temperature), benthic metabolism in mussel beds is mediated by mussel species traits including biomass, excretion, and thermal tolerance; H2) thermally sensitive species have stronger impacts than tolerant species on benthic metabolism in the late summer but not the autumn because thermally sensitive species have stronger ecophysiological and behavioral responses to increased temperatures; H3) after accounting for mussel respiration, background benthic ER is higher in the presence of more-mobile mussels because of increased bioturbation. Finally, we sought to characterize the overall patterns in mussel-driven net zoogeochemical effects on benthic CO_2 exchange across the experiment.

METHODS

We conducted an in situ field experiment using self-contained metabolic incubation chambers under contrasting environmental conditions in the late summer and the autumn in the Sipsey River, an undammed, 5th-order tributary of the Tombigbee River in western Alabama, USA. The Sipsey River hosts a diverse and abundant mussel fauna, including most of its historical species richness (McCullagh et al. 2002, Haag and Warren 2010). The surrounding watershed is largely forested with extensive floodplain wetlands and low background nutrient concentrations (Atkinson et al. 2019). The study site was an ~50-m reach of a shallow run with gravel and sand substrate.

Experimental design

Our experimental design featured 39 self-contained metabolic chambers. The construction and installation of the chambers is described in detail in Appendix S1. Briefly, each

chamber consisted of a tubular PVC base (radius = 0.254 m) and a removable hemispheric acrylic dome of equal radius. We installed the chamber bases between 6 July and 24 August 2023 by burying them flush with the sediment surface along a series of 23 lateral transects that were ~2 m apart. We placed 2 chamber bases ~2.5 m apart along most transects. The 4 transects furthest downstream only had 1 chamber because hydraulic forces prevented installation in some portions of these transects.

We removed all mussels present at the installation locations prior to burying the metabolic chamber bases. Each chamber was randomly assigned either as a control with no mussels restocked (n = 7) or as 1 of 4 species treatments (n = 8 each). We restocked the treatment chambers with 7 individuals from 1 of 4 different mussel species with contrasting traits (Fig. 1A): *Amblema plicata* (Say, 1817) (large, thermally tolerant, moderate excretion rates), *Fusconaia cerina* (Conrad, 1838) (small, thermally tolerant, low excretion rates), *Lampsilis ornata* (Conrad, 1835) (large, thermally sensitive, high excretion rates), and *Pustulosa kieneriana* (Lea, 1852) (small, thermally sensitive, moderate excretion rates) (Atkinson et al. 2020a, b, van Ee et al. 2022). These are common species that represent a cross section of the phylogenetic and functional diversity of the Sipsey River mussel fauna (Atkinson et al. 2020b). All mussels were restocked from the same site where the experiment was conducted. The resulting density (35 ind./m^2) is reflective of a high-density patch in a healthy mussel bed in the Sipsey River (Haag and Warren 2010, Atkinson and Forshay 2022). We also measured the length of each mussel and estimated their biomass using length–mass equations taken from Atkinson et al. (2020a).

Benthic metabolism

Incubations After installation, we left the chamber bases undisturbed for at least 2 wk for sediment conditions to equilibrate before conducting benthic metabolism incubations. We performed incubations by sequentially affixing the chamber domes to each of the buried bases to create fluid-tight chambers (Appendix S1, Fig. 1B). To calculate benthic metabolic rates, we conducted 2 sets of incubations: 1 in late summer (19–28 September) and 1 in autumn (23–27 October) of 2023.

Before, during, and after both the late-summer and autumn incubation periods, we visually checked all chambers for mortality. We also re-collected all mussels from each chamber at the end of the late-summer incubations, verified their identities, and replaced them. When we observed mortality before an incubation period, we carefully replaced the deceased mussel with a live mussel of the same species so as to minimize disturbance to the sediment. When we observed mortality after an incubation period, we removed any recorded deceased mussels from the biomass estimates for their respective chambers. All mortality occurred before or during the late-summer incubation. In total, 15 mussels (~7%) died during this period. Of these mussels, 11 were located and replaced at least 2 d prior to the late-summer incubations. The other 4 were located and replaced on the day of their respective chamber incubations. We were also unable to locate 2 mussels during the verification check after the late-summer incubations, so these mussels were not included in biomass calculations. Given the rarity of mortality and the fact that most deceased mussels were removed and replaced well in advance of the incubations, we assume that any impact of mussel tissue decomposition on our results was negligible.

The late-summer incubations were characterized by warmer incubation temperatures (23.8–25.0°C) and higher flows at the nearest United States Geological Survey stream gauge #02446500 (mean daily discharge = 1.69–1.93 m^3/s) than the autumn incubations, which had

cooler incubation temperatures (17.7–19.3°C) and slightly lower flows (1.56–1.73 m^3/s). We placed a Hobo® dissolved O_2 (DO) data logger (U26-001; Onset® Computer Corporation, Bourne, Massachusetts), a recirculating pump (flow rate = 1 L/min), and a Hobo Pendant Temp/Light 64K data logger (UA-002-64; Onset Computer Corporation) into each chamber (Fig. 1B). We set loggers to record DO, light, and temperature values every minute. We truncated water temperature and light intensity data to match the interval of O_2 flux curves (see "Metabolic rate calculations" below). During each incubation period, we assembled 4 PAR calibration chambers containing both a Pendant and a PME miniPAR logger (Precision Measurement Engineering, Vista, California). The Temp/Light loggers record light intensity values, which scale nonlinearly with PAR. We used the PAR calibration chambers to generate an asymptotic curve estimating PAR from light intensity (Long et al. 2012). We used the PAR calibration chamber data to conduct a nonlinear least squares regression to estimate PAR from light intensity (Fig. S1; Long et al. 2012) (R package *drc*, version 3.0.1; Ritz et al. 2015) in R statistical software (version 4.2.3; R Project for Statistical Computing, Vienna, Austria).

During each incubation period, we conducted 6 to 9 incubations daily, depending on the number of people on the field crew that day. This meant we were conducting incubations over several days, so we randomized the order in which we conducted these incubations. Each incubation lasted 4 h, and incubations were started serially (i.e., after 1 incubation was started, we immediately started the next). For the first 2 h, we used 100% light-blocking greenhouse shade cloth to halt primary production and isolate benthic ER. This 2-h dark period ensured sufficient change in O_2 concentrations to calculate ER. After the dark period, the tarp was removed, allowing primary production to resume for an additional 2 h. One limitation imposed by these incubation methods is that bivalves are known to close their shells in response to

darkness or shadows (Wilkens 2008). The impacts that this shadow response has on metabolism is unknown; however, some mussel species show variation in filtration behavior in response to darkness (Hills et al. 2020, Pouil et al. 2021). As such, we cannot rule out the possibility that mussel impacts on metabolism vary among light and dark conditions, and the results of the present study should be interpreted with this caveat in mind.

Metabolic rate calculations We calculated ER and GPP using time series O_2 concentration data collected by the DO loggers during each incubation. We split the resulting dataset into light and dark incubations, then conducted local linear regression analyses on the resulting O_2 flux curves (package *LoLinR*, version 0.0.0.9000; Olito et al. 2017). Local linear regression reduces bias and increases accuracy in the estimation of monotonic biological rates by identifying the slope of the most linear subset of a time series, reducing the need for potentially subjective measures such as manual data truncation (Olito et al. 2017, Roth et al. 2019). The *LoLinR* package (function rankLocReg) requires the user to set a minimum proportion (α) of the total number of observations in the time series (N) to be used in the analysis. At minimum, $\alpha \times N \geq 15$. In our dataset, N was ~120 min, so we used $\alpha = 0.3$ (30% of the dataset or 40 min). However, our data still required manual truncation in the presence of saturation effects or when noise or sensor failures occurred near the middle of an incubation. In such cases, we removed the problematic portion of the time series and reran the analysis ($n = 64$ of 156 total incubations). The shortest truncated time series were 15 min long to capture the initial increase in DO that occurred prior to DO saturation in some chambers. We were unable to isolate a linear signal from 1 light incubation. The slopes of the O_2 fluxes, standardized for chamber volume and surface area (g O_2 m^{-2} h^{-1}) represented ER in dark incubations and net ecosystem productivity (NEP) in light

incubations. We calculated GPP as NEP + ER.

Variation in metabolism among treatments and between seasons We fit separate exploratory 2-way analysis of variance (ANOVA) models to characterize variation in ER and GPP within and among species treatments and seasons (late summer vs autumn). We conducted pairwise post hoc tests using estimated marginal means (EMM) with Tukey-adjusted *p*-values (R package *emmeans*, version 1.10.3; Lenth 2023). This analysis was intended only to test for overall differences, not to identify the drivers of that variation or test our hypotheses. We determined that the models conformed to the assumptions of homogeneity of variance and appropriate residual distributions based on scale-location plots and histograms.

Nutrient excretion and sediment organic matter

In between the late-summer and autumn incubations, we quantified mussel excretion rates and sediment organic matter content. We measured N (as NH_4^+-N) and P (as soluble reactive P) excretion rates for 1 randomly selected mussel from each incubation chamber while ambient water temperatures were at 23.9°C (see Appendix S1 for detailed methods). We multiplied those excretion rates by the total mussel biomass in each chamber to estimate total hourly N and P excretion for each chamber (Fig. S2). On 9 October 2023, we collected a sediment core from the center of each chamber (depth = 20 cm, volume = 912 cm^3), placed the cores on ice, and returned them to the lab. Immediately upon removing the sediment cores, we replaced the removed sediments by hand with sediments adjacent to the incubation bases and allowed these sediments to re-equilibrate in between the late-summer and autumn incubations. Sediment cores were dried to a constant mass at 60°C for a minimum of 48 h. We then took a

homogenized subsample of each core to determine organic matter content. We weighed each subsample to determine dry mass (DM) and then combusted them at 550°C for 6 h. After combustion, subsamples were weighed to calculate ash-free dry mass (AFDM). We sampled excretion and sediment cores once between the late-summer and autumn incubations and assume that our measurements are representative of patterns in both incubation periods. Finally, we determined sediment organic matter content (%OM) based on sediment DM and AFDM values, where %OM = 100(DM – (AFDM / DM)).

Effects of mussel ecophysiological traits on benthic metabolism

We identified the potential drivers of variation within and among treatments by modeling the effects of biomass, thermal tolerance, and nutrient excretion on benthic metabolism (H1, H2) with linear mixed-effects models (LMM) (R package *lme4*, version 1.1.35.5; Bates et al. 2015). Our models also included environmental covariates that have proximate impacts on benthic metabolism: temperature, PAR, and %OM. Testing specific drivers allowed us to identify sources of variation that might be masked when conducting simple categorical comparisons that do not account for environmental covariates or species traits. We tested whether fixed effects improved model fit using Type II Wald chi-square tests (R package *car*, version 3.1.2; Fox and Weisberg 2019). We also refit all LMM with scaled and centered fixed effects to derive standardized coefficient estimates ($\hat{\beta} \pm$ SE) as a measure of effect size for fixed effects with p-values < 0.05. $\hat{\beta}$ estimates should be interpreted as the relative strength of the relationship of each fixed effect to the response variable when all other fixed effects are at their means. Our LMM analyses included all experimental and control chambers as observations.

To test how mussel biomass, thermal tolerance, and nutrient excretion affected benthic

metabolism (H1), we constructed 2 models with log-transformed ER and GPP as the respective response variables. Thermal tolerance was coded as a categorical fixed effect (sensitive, tolerant, or control), and all other fixed effects were coded as continuous variables. We addressed H2 by including an interaction term between thermal tolerance and temperature to determine whether there were any seasonal differences for effects of thermal tolerance on ER or GPP. We included chamber as a random intercept to account for repeated measures across seasons. The ER model was structured as

$$\log \mathrm{ER} \sim \mathrm{biomass} + \mathrm{sediment\ \%OM} + \mathrm{thermal\ tolerance} \times \mathrm{mean\ dark\ incubation\ temperature} + (1 \mid \mathrm{chamber}).$$

The GPP model was structured as

$$\log \mathrm{GPP} \sim \mathrm{N\ excretion} + \mathrm{P\ excretion} + \mathrm{mean\ PAR} + \mathrm{thermal\ tolerance} \times \mathrm{mean\ light\ incubation\ temperature} + (1 \mid \mathrm{chamber}).$$

We determined that all models in the parametric analyses, including subsequent analyses, conformed to the assumptions of no multicollinearity, homogeneity of variance, and appropriate residual distributions based on variance inflation factors, scale-location plots, and histograms, respectively.

Potential nutrient limitation of algal accrual To place potential excretion effects into context, we analyzed data from a previously unpublished nutrient limitation study conducted in September 2016 to assess nutrient limitation, following methods in Atkinson et al. (2013). The aim of this analysis was to determine whether benthic algal accrual was limited by nutrient availability in the Sipsey and, consequently, whether mussel excretion was likely to increase benthic primary production and thereby alter metabolism. Briefly, we used nutrient diffusing

substrates (NDS) to assess whether benthic algae accrual was either limited by N or P or co-limited by both nutrients. Each NDS consisted of a series of 30-mL cups filled with 2% agar solution and additions of NO_3^- (N; 0.5 M $NaNO_3$), PO_4^{3-} (P; 0.5 M KH_2PO_4), N + P (NP; 0.5 M $NaNO_3$ + 0.5 M KH_2PO_4), or control (C) treatments of agar alone. Each cup was capped with a fritted glass disk as a substrate for algal accrual and secured to an L-bar. We deployed 9 replicates of each treatment (N, P, NP, C) at 11 sites in the Sipsey River with variable mussel densities. We categorized sites with clearly defined mussel aggregations and densities >15 ind./m^2 as high-mussel sites (n = 6) and sites with no clear aggregation and mussel densities <15 ind./m^2 as low-mussel sites (n = 5). We allowed the NDS to incubate for 18 d before collection, then removed the fritted disks, placed them on ice, and transported them to the lab. We extracted chlorophyll *a* (Chl *a*) from the disks in acetone and quantified Chl *a* concentrations with spectrophotometric methods (Steinman et al. 2017).

We then analyzed algal accrual (Chl *a*) data with an LMM with treatment, mussel presence, and treatment × mussel interaction as fixed effects and site as a random effect (R package *lme4*). We used EMM with Tukey-adjusted p-values to test the response of Chl *a* accrual to nutrient addition treatments at high-mussel and low-mussel sites (R package *emmeans*).

Burrowing behavior

To quantify mussel movement behavior, we tagged each mussel with a unique 3-digit identification number. We affixed a shellfish tag (Floy Tag and Manufacturing, Inc., Seattle, Washington) displaying the identifier and a segment of fly line with a waterproof paper tag bearing the same identifier to the shell of each mussel. Once/wk for 4 wk (5–27 September), we conducted movement surveys to identify the position of each mussel in each chamber.

We quantified horizontal movement by placing a circular aluminum grid with square cells over the entire area of each chamber base (Fig. 1C). Each cell was labeled using a row–column coordinate system. We locked the grids into place in the same position each week and recorded the coordinates where each mussel was found. We created a horizontal movement index by summing the number of grid cells traveled both row-wise and column-wise during each week for each mussel. When mussels were found on the border of 2 cells, we indexed their movement as ½ a cell.

We quantified vertical movement based on the proportion of mussels in each species that moved vertically. Each week, we recorded whether each mussel was visible at the surface or buried. If a mussel went from buried in the previous week to the surface in the next week, or vice versa, it was assigned a score of 1. If it stayed at the surface or buried between consecutive weeks, it was assigned a score of 0. For mussels that were buried, we measured the length of the fly line that was visible above the sediment surface and calculated burial depth as the difference between that length and the total length of the attached fly line.

To test whether differences in the magnitude and frequency of horizontal and vertical movement by mussels differed by species and thermal tolerance, we used extensions of the linear model framework. We tested whether horizontal movement differed between species and thermal tolerances by applying an aligned rank transform (ART) to the horizontal movement index and using nonparametric 1-way ANOVA (R package *ARTool,* version 0.11.1; Wobbrock et al. 2011). Species and thermal tolerance were factors in their respective models, and tag number was a random error term in these models to account for repeated measures. Then, we used generalized linear mixed-effects models (GLMM; R package *lme4*) to test whether vertical movement frequency differed between species and thermal tolerance groups, with species or thermal

tolerance as a fixed effect and tag number as a random effect (binomial family, logit link). We obtained *p*-values for GLMM fixed effects using Wald *z* statistics. Finally, we tested whether burial depth differed between species and thermal tolerances by again applying ART ANOVA for both species and thermal tolerance with tag number as a random error term. We conducted pairwise post hoc tests using EMM with Tukey-adjusted *p*-values for GLMM (R package *emmeans*) and ART-C contrasts for ART ANOVA (Elkin et al. 2021).

Indirect effects of mussel burrowing behavior on benthic metabolism To test for potential indirect mussel-driven bioturbation effects on background benthic ER (H3), we first used lab-calculated respiration rates to approximate the proportion of ER driven by mussel respiration during the late-summer incubation period. We used WebPlotDigitizer (version 4.6; A. Rohtgi, Automeris.io; https://automeris.io) to extract mass-specific respiration rates for the 4 study species at 20 and 30°C (van Ee et al. 2022). The mean late-summer incubation temperature was 24.1°C, so we averaged the respiration rates calculated at 20 and 30°C for each species to infer respiration rates at ~25°C. We use these rates as estimates only because laboratory-measured rates may not exactly replicate in situ respiration rates because of the inherent physiological and behavioral constraints faced by organisms in microcosms. We multiplied mass-specific rates by the total mussel biomass in each chamber and subtracted the resultant value from total benthic ER to yield an estimate of background benthic ER for each chamber. Then we used a model-selection approach to identify whether the movement variables we assessed were likely to explain variation in background ER (R package *MuMIn*, version 1.48.4; Bartoń 2023). The data for the model selection procedure included only complete cases with nonmissing values for all variables. The global model was a multiple regression with log-transformed background ER as

the response variable, structured as

$$\log \mathrm{ER} \sim (\text{mean horizontal movement} + \text{mean vertical movement} + \text{mean burial depth}) \times \text{mean dark incubation temperature} + \text{sediment \%OM}.$$

We present only models within $\Delta\mathrm{AICc} \leq 2$ of the top model. We used the model with the highest adjusted R^2 to hypothesize which terms were most strongly associated with variation in background ER based on Type II F tests of the model terms and $\hat{\beta}$ estimates.

Net zoogeochemical effect

To quantify the relative impact that mussels had on benthic C exchange in our experiment, we converted O_2 fluxes to CO_2, assuming a 1:1 molar respiration quotient. We then calculated % change in mean CO_2 exchange between each species treatment relative to the control in both seasons. Positive % change values represented a mean increase in benthic CO_2 uptake relative to the controls, whereas negative values represented increased CO_2 efflux.

RESULTS

Mussel biomass, thermal tolerance, and nutrient excretion affect benthic metabolism

Benthic ER ranged from 0.0303 to 0.2090 g O_2 m^{-2} h^{-1} in late summer and from 0.0188 to 0.0914 mg O_2 m^{-2} h^{-1} in autumn. ER differed among species treatments ($F_{4,68} = 8.0$, $p < 0.0001$) and season ($F_{1,68} = 14.1$, $p < 0.0001$), but there was no species × season interaction ($F_{4,68} = 1.1$, $p = 0.3$; Table S1, Fig. 2A). ER was best explained by increased mussel biomass ($\hat{\beta} = 0.364 \pm 0.121$), increased dark incubation temperature ($\hat{\beta} = 0.176 \pm 0.178$), and the presence of thermally tolerant ($\hat{\beta} = 0.327 \pm 0.330$) or thermally sensitive ($\hat{\beta} = 0.794 \pm 0.338$) mussels but was not explained by sediment %OM or the tolerance × temperature interactions (Tables 1, S2,

Fig. 2B).

Benthic GPP ranged from 0.0740 to 0.3950 mg O_2 m^{-2} h^{-1} in late summer and from 0.0788 to 0.6600 g O_2 m^{-2} h^{-1} in autumn. GPP differed among species treatments ($F_{4,67} = 4.0$, $p = 0.006$) and season ($F_{1,67} = 4.9$, $p = 0.03$), but there was no species × season interaction ($F_{4,67} = 0.5$, $p = 0.8$; Table S3, Fig. 2C). GPP was best explained by increasing N excretion ($\hat{\beta} = 0.550 \pm 0.220$), decreasing P excretion ($\hat{\beta} = -0.420 \pm 0.199$), and decreasing light incubation temperature ($\hat{\beta} = -0.203 \pm 0.188$), but not by PAR, thermal tolerance, or the tolerance × temperature interaction (Tables 1, S4, Fig. 2D).

Chl *a* concentrations from the 2016 NDS study were best explained by nutrient treatment ($\chi^2 = 25.3$, $p < 0.0001$, df = 3) and the nutrient × mussel interaction ($\chi^2 = 31.9$, $p < 0.0001$, df = 3) but not mussel presence alone ($\chi^2 = 0.4$, $p = 0.5$, df = 1). Chl *a* was higher on all nutrient addition treatments than controls at high-mussel sites but only increased on the NP treatment at low-mussel sites (Table S5, Fig. 3).

Vertical movement and burial depth depend on species identity and thermal tolerance

Horizontal movement did not differ between species treatments ($F_{3,131} = 1.0$, $p = 0.4$; Table S6, Fig. 4A) or thermal tolerance treatments ($F_{1,133} = 0.3$, $p = 0.6$; Table S7, Fig. 4B). However, vertical movement frequency did differ between species ($\chi^2 = 22.4$, $p < 0.0001$, df = 3; Table S8, Fig. 4C). Vertical movement also differed with thermal tolerance ($\chi^2 = 6.6$, $p = 0.01$, df = 1; Table S9), with thermally sensitive species tending to bury or unbury more frequently ($z = 2.6$, $p = 0.01$, df = 1; Fig. 4D). Burial depth varied between species ($F_{3,196} = 40.8$, $p < 0.0001$; Table S10, Fig. 4E) and thermal tolerances ($F_{1,198} = 70.9$, $p < 0.0001$; Table S11), with thermally sensitive species tending to bury deeper than thermally tolerant species ($t = 8.4$, $p < 0.0001$, df =

198; Fig. 4F).

Bioturbation is associated with increased ER

Among the top models of background ER as a function of movement, the most common explanatory variables were mean horizontal movement ($n = 6$) and mean burial depth ($n = 6$), followed by mean vertical movement ($n = 2$), mean dark incubation temperature ($n = 2$), and the burial depth × temperature interaction ($n = 1$; Table 2).

The most variation in background ER was explained by a model including mean burial depth, mean dark incubation temperature, weekly mean horizontal movement, and the burial depth × temperature interaction ($F_{4,25} = 2.7$, $p = 0.06$, $R^2_{adj} = 0.19$; Table 2, Fig. 5). Background ER was best explained by increased horizontal movement ($F_{1,25} = 5.1$, $p = 0.03$; $\hat{\beta} = 0.519 \pm 0.188$; Tables S12, S13, Fig. 5). The other terms in the model generally had positive associations with background ER but did not explain variation well (burial depth: $F_{1,25} = 2.0$, $p = 0.2$, $\hat{\beta} = 0.305 \pm 0.170$; temperature: $F_{1,25} = 0.2$, $p = 0.7$, $\hat{\beta} = 0.216 \pm 0.175$; burial depth × temperature interaction: $F_{1,25} = 3.3$, $p = 0.08$, $\hat{\beta} = -0.390 \pm 0.213$; Tables S12, S13, Fig. 5).

Net zoogeochemical effect on C exchange varies between species and seasons

Relative change in benthic CO_2 flux across species treatments ranged from –45.1 to 62.9% in the late summer and from –18.5 to 104.0% in the autumn (Fig. 6). On average, *A. plicata* and *P. kieneriana* were associated with increases in CO_2 uptake in both late summer and autumn. The magnitude of this increase was larger for *A. plicata* in the autumn than the late summer but similar between seasons for *P. kieneriana*. *Fusconaia cerina* was associated with a relatively small increase in CO_2 efflux in both seasons. *Lampsilis ornata* was associated with

increased CO_2 efflux in the late summer but an increased uptake in the autumn, making it the only species that had different directionality in its average zoogeochemical effects between seasons.

DISCUSSION

We sought to determine which species traits were most important in mediating the impacts of freshwater mussels on benthic metabolism. Our findings support a growing body of evidence that animals can have strong impacts on C cycling in freshwater ecosystems (Schindler et al. 1997, Hall et al. 2003, Atwood et al. 2013, Atkinson et al. 2018, Nummi et al. 2018). Biomass and thermal tolerance traits regulated the strength of mussel direct impacts on ER, whereas variation in excretion and movement behavior were associated with indirect changes to GPP and ER. These direct and indirect mechanisms contributed to substantial interspecific variation in the average zoogeochemical effects of mussels on benthic C exchange. The magnitude of the zoogeochemical effects in this study suggests that animals can have strong effects on stream C cycles. Further, animal biogeochemical contributions should not be overlooked, and linkages between animal conservation and biogeochemistry should continue to be explored.

As expected, the differences in benthic metabolism that we observed were associated with mussel species traits and with light and temperature (H1). Increasing mussel biomass led to higher ER because of the inherent relationship between body size and organismal metabolic rates (Brown et al. 2004). Mussel biomass had a stronger effect on ER in our experiment than increased temperature, although the SEs of the respective $\hat{\beta}$ estimates overlapped. Mussel-driven N excretion was positively associated with GPP, and NDS results suggested that sites with

mussels may be limited by N or P or co-limited by both nutrients. We speculate that the site may be N limited, and mussels may promote benthic algal production there by alleviating nutrient limitation, as has been documented in other systems (Allen et al. 2012, Atkinson et al. 2013, Lopez et al. 2020). Surprisingly, P excretion was negatively associated with GPP. It is difficult to surmise a biological reason for a negative relationship between P and GPP, so it is possible this apparent relationship is a statistical or stoichiometric artifact. For example, *L. ornata* had much higher P excretion than *A. plicata* but similar N excretion and considerably lower GPP—perhaps the contrast in P excretion between species influenced the coefficient estimates, but N excretion is more important from a biological standpoint. The observed increase in GPP as temperatures declined in the autumn was likely driven by the extended period of low flow that occurred during our experiment because benthic filamentous algae and Chl *a* tend to accrue between scouring flows (Francoeur and Biggs 2006, Davie 2012). Algal assemblage sampling was beyond the scope of this study, but we observed substantial filamentous algae accrual as flow decreased between late summer and autumn, likely increasing GPP despite the ~6°C decrease in water temperature.

Our findings also suggest that thermally sensitive species can have disproportionate zoogeochemical effects on stream ecosystems even after accounting for biomass (H2). Van Ee et al. (2022) modeled NH_3 excretion for thermally sensitive and thermally tolerant species from the Sipsey River across a seasonal temperature gradient and found that at low (10°C) to moderate (20°C) temperatures, the contributions of sensitive species to ER were proportionally similar to their biomass in the assemblage; however, at high temperatures (30°C), the effects of sensitive species increased by an additional 13.7 to 15.2%. In our study, the mean impact of thermally sensitive species on ER was over 2× stronger than the impact of tolerant species. This result

supports other evidence that the relative abundance of thermally sensitive taxa can fundamentally alter stream ecosystem function (Spooner and Vaughn 2008, Vaughn et al. 2008).

The frequency and depth of vertical movement by mussels also varied with thermal tolerance, but horizontal movement did not. The tendency of thermally sensitive species to bury deeper and move between the surface and subsurface with higher frequency supports the hypothesis that these species respond to temperature both physiologically and behaviorally (Gough et al. 2012). Variability in movement may indirectly increase background rates of benthic ER via bioturbation (H3). Horizontal movement and burial depth were included in most models we tested to identify relationships between movement and background ER, suggesting these variables may mediate the strength of mussel bioturbation effects. If the hypothesis that mussel movement increases ER via bioturbation is true, thermally sensitive species may have not only stronger direct effects than tolerant species on total benthic ER in mussel aggregations, but also stronger indirect effects. Thermally sensitive species are substantially more vulnerable to drought and warming than tolerant species (Allen et al. 2013, Atkinson et al. 2014, Lopez et al. 2022). Thus, as climate change drives the loss of thermally sensitive species from mussel aggregations, there will likely be fundamental changes to stream ecosystem function in areas where mussels have strong zoogeochemical impacts.

Our comparison of changes in benthic CO_2 exchange suggests that the direct and indirect effects of mussels integrate to drive detectable changes in stream C cycles. However, we can only speculate on which traits may be associated with CO_2 uptake vs efflux because the species that were associated with similar changes in CO_2 exchange had some contrasting traits. The explanation for how mussels mediated benthic CO_2 exchange may lie in the balance between the direct and indirect impacts of mussels on ER and their indirect impacts on GPP. Whether mussels

are associated with CO_2 uptake or efflux should depend on whether they promote enough growth—and thereby CO_2 uptake—by benthic algae via habitat provisioning and nutrient recycling to outpace the CO_2 efflux they generate via respiration and bioturbation. Whether net uptake or efflux is the result should therefore be determined by species traits. For example, mussels that are large and have more complex morphology (e.g., ridges or bumps) or do not bury, such as *A. plicata*, may provide more substrate for algal accrual, leading to higher CO_2 uptake when environmental conditions favor filamentous algae (Spooner and Vaughn 2006). On the other hand, the effects of thermally sensitive species, such as *L. ornata*, may depend on the animal's physiological and behavioral responses to temperature, which vary seasonally, with corresponding variation in benthic CO_2 exchange.

Variation in stream metabolism ultimately drives important changes in freshwater C fluxes (Hotchkiss et al. 2015, Hall et al. 2016, Maranger et al. 2018). Beyond predicting changes in freshwater C dynamics, an improved understanding of how animals affect stream metabolism creates interdisciplinary synergy between biogeochemistry and conservation (Schmitz et al. 2014, 2018). New ways of thinking recognize that animal conservation can help address the dual challenges of biodiversity conservation and climate change mitigation through animal-driven C storage (Schmitz et al. 2014, Urban 2015). Yet, to our knowledge, these approaches have largely been applied to terrestrial systems. Therefore, quantifying and determining the mechanisms underlying strong zoogeochemical effects on stream metabolism and accounting for these effects in conservation plans should be considered an emerging priority in freshwater science.

ACKNOWLEDGEMENTS

Author contributions: All authors contributed to study design and conceptualization. CLA designed the incubation chambers and directed the 2016 nutrient diffusing substrate study. JWL and MBL led the fieldwork. JWL led the data analysis and wrote the initial draft of the manuscript with input from all authors.

We thank the Weyerhauser Company for providing access to our field site. We thank Tayton Alvis, Ian Brunetz, Jacob Dorris, Garrett Hopper, Taylor Kelley, Caleb Kennedy, Lauren Morris, Irene Sánchez González, Chelsea Smith, and Nate Sturm for assistance with fieldwork. James Pugh and the University of Alabama College of Arts and Sciences Machine Shop constructed the chamber based on designs specified by CLA. The National Science Foundation provided funding support for this project (DEB-1942707 and DBI-2305574), and freshwater mussel collection was conducted under Alabama Department of Conservation and Natural Resources permit #2023126032468680.

Data availability statement: The data collected during this study are publicly available at https://figshare.com/s/6e81d2514ef05d502549.

LITERATURE CITED

Allen, D. C., H. S. Galbraith, C. C. Vaughn, and D. E. Spooner. 2013. A tale of two rivers: Implications of water management practices for mussel biodiversity outcomes during droughts. Ambio 42:881–891.

Allen, D. C., and C. C. Vaughn. 2009. Burrowing behavior of freshwater mussels in experimentally manipulated communities. Journal of the North American Benthological Society 28:93–100.

Allen, D. C., C. C. Vaughn, J. F. Kelly, J. T. Cooper, and M. H. Engel. 2012. Bottom-up biodiversity effects increase resource subsidy flux between ecosystems. Ecology 93:2165–2174.

Atkinson, C. L., and K. J. Forshay. 2022. Community patch dynamics governs direct and indirect nutrient recycling by aggregated animals across spatial scales. Functional Ecology 36:595–606.

Atkinson, C. L., J. P. Julian, and C. C. Vaughn. 2014. Species and function lost: Role of drought in structuring stream communities. Biological Conservation 176:30–38.

Atkinson, C. L., T. B. Parr, B. C. van Ee, D. D. Knapp, M. Winebarger, K. J. Madoni, and W. R. Haag. 2020a. Length-mass equations for freshwater unionid mussel assemblages: Implications for estimating ecosystem function. Freshwater Science 39:377–390.

Atkinson, C. L., B. J. Sansom, C. C. Vaughn, and K. J. Forshay. 2018. Consumer aggregations drive nutrient dynamics and ecosystem metabolism in nutrient-limited systems. Ecosystems 21:521–535.

Atkinson, C. L., B. C. van Ee, Y. Lu, and W. Zhong. 2019. Wetland floodplain flux: Temporal and spatial availability of organic matter and dissolved nutrients in an unmodified river.

Biogeochemistry 142:395–411.

Atkinson, C. L., B. C. van Ee, and J. M. Pfeiffer. 2020b. Evolutionary history drives aspects of stoichiometric niche variation and functional effects within a guild. Ecology 101:e03100.

Atkinson, C. L., and C. C. Vaughn. 2015. Biogeochemical hotspots: Temporal and spatial scaling of the impact of freshwater mussels on ecosystem function. Freshwater Biology 60:563–574.

Atkinson, C. L., C. C. Vaughn, K. J. Forshay, and J. T. Cooper. 2013. Aggregated filter-feeding consumers alter nutrient limitation: Consequences for ecosystem and community dynamics. Ecology 94:1359–1369.

Atwood, T. B., E. Hammill, H. S. Greig, P. Kratina, J. B. Shurin, D. S. Srivastava, and J. S. Richardson. 2013. Predator-induced reduction of freshwater carbon dioxide emissions. Nature Geoscience 6:191–194.

Atwood, T. B., E. M. P. Madin, A. R. Harborne, E. Hammill, O. J. Luiz, Q. R. Ollivier, C. M. Roelfsema, P. I. Macreadie, and C. E. Lovelock. 2018. Predators shape sedimentary organic carbon storage in a coral reef ecosystem. Frontiers in Ecology and Evolution 6:110.

Bartoń, K. 2023. *MuMIn*: Multi-model inference. (Available from: https://CRAN.R-project.org/package=MuMIn)

Bates, D., M. Mächler, B. M. Bolker, and S. C. Walker. 2015. Fitting linear mixed-effects models using lme4. Journal of Statistical Software 67(1):1–48.

Brown, J. H., J. F. Gillooly, A. P. Allen, V. M. Savage, and G. B. West. 2004. Toward a metabolic theory of ecology. Ecology 85:1771–1789.

Cole, J. J., Y. T. Prairie, N. F. Caraco, W. H. McDowell, L. J. Tranvik, R. G. Striegl, C. M.

Duarte, P. Kortelainen, J. A. Downing, J. J. Middelburg, and J. Melack. 2007. Plumbing the global carbon cycle: Integrating inland waters into the terrestrial carbon budget. Ecosystems 10:171–184.

Curley, E. A. M., R. Thomas, C. E. Adams, and A. Stephen. 2022. Adaptive responses of freshwater pearl mussels, *Margaritifera margaritifera*, to managed drawdowns. Aquatic Conservation: Marine and Freshwater Ecosystems 32:466–483.

Davie, A. 2012. Succession and accrual of benthic algae on cobbles of an upland river following scouring. Inland Waters 2:89–100.

Dirzo, R., H. S. Young, M. Galetti, G. Ceballos, N. J. B. Isaac, and B. Collen. 2014. Defaunation in the Anthropocene. Science 345:401–406.

Elkin, L. A., M. Kay, J. J. Higgins, and J. O. Wobbrock. 2021. An aligned rank transform procedure for multifactor contrast tests. Pages 754–768 *in* J. Nichols, R. Kumar, and M. Nebeling (editors). UIST '21: The 34th Annual ACM Symposium on User Interface Software and Technology. Association for Computing Machinery, virtual event, USA.

Fox, J., and S. Weisberg. 2019. An R companion to applied regression. 3rd edition. Sage Publications, Inc., Thousand Oaks, California.

Francoeur, S. N., and B. J. F. Biggs. 2006. Short-term effects of elevated velocity and sediment abrasion on benthic algal communities. Hydrobiologia 561:59–69.

Gough, H. M., A. M. Gascho Landis, and J. A. Stoeckel. 2012. Behaviour and physiology are linked in the responses of freshwater mussels to drought: Differential mussel responses to drought. Freshwater Biology 57:2356–2366.

Haag, W. R., and M. L. Warren. 2010. Diversity, abundance, and size structure of bivalve assemblages in the Sipsey River, Alabama. Aquatic Conservation: Marine and Freshwater

Ecosystems 20:655–667.

Hall, C. A. S. 1972. Migration and metabolism in a temperate stream ecosystem. Ecology 53:585–604.

Hall, R. O., J. L. Tank, M. A. Baker, E. J. Rosi-Marshall, and E. R. Hotchkiss. 2016. Metabolism, gas exchange, and carbon spiraling in rivers. Ecosystems 19:73–86.

Hall, R. O., J. L. Tank, and M. F. Dybdahl. 2003. Exotic snails dominate nitrogen and carbon cycling in a highly productive stream. Frontiers in Ecology and the Environment 1:407–411.

Hills, A., S. Pouil, D. Hua, and T. J. Mathews. 2020. Clearance rates of freshwater bivalves *Corbicula fluminea* and *Utterbackia imbecillis* in the presence and absence of light. Aquatic Ecology 54:1059–1066.

Hopper, G. W., S. Chen, I. Sánchez González, J. R. Bucholz, Y. Lu, and C. L. Atkinson. 2021. Aggregated filter-feeders govern the flux and stoichiometry of locally available energy and nutrients in rivers. Functional Ecology 35:1183–1195.

Hotchkiss, E. R., R. O. Hall, R. A. Sponseller, D. Butman, J. Klaminder, H. Laudon, M. Rosvall, and J. Karlsson. 2015. Sources of and processes controlling CO_2 emissions change with the size of streams and rivers. Nature Geoscience 8:696–699.

Lenth, R. V. 2023. *emmeans*: Estimated marginal means, aka least-squares means. (Available from: https://cran.r-project.org/package=emmeans)

Long, M. H., J. E. Rheuban, P. Berg, and J. C. Zieman. 2012. A comparison and correction of light intensity loggers to photosynthetically active radiation sensors. Limnology and Oceanography: Methods 10:416–424.

Lopez, J. W., T. P. DuBose, A. J. Franzen, C. L. Atkinson, and C. C. Vaughn. 2022. Long-term

monitoring shows that drought sensitivity and riparian land use change coincide with freshwater mussel declines. Aquatic Conservation: Marine and Freshwater Ecosystems 32:1571–1583.

Lopez, J. W., T. B. Parr, D. C. Allen, and C. C. Vaughn. 2020. Animal aggregations promote emergent aquatic plant production at the aquatic–terrestrial interface. Ecology 101: e03126.

Maranger, R., S. E. Jones, and J. B. Cotner. 2018. Stoichiometry of carbon, nitrogen, and phosphorus through the freshwater pipe. Limnology and Oceanography Letters 3:89–101.

Matisoff, G., J. B. Fisher, and S. Matis. 1985. Effects of benthic macroinvertebrates on the exchange of solutes between sediments and freshwater. Hydrobiologia 122:19–33.

McCullagh, W. H., J. D. Williams, S. W. McGregor, J. M. Pierson, and C. Lydeard. 2002. The unionid (Bivalvia) fauna of the Sipsey River in northwestern Alabama, an aquatic hotspot. American Malacological Bulletin 17:1–15.

McInnes, P. F., R. J. Naiman, J. Pastor, and Y. Cohen. 1992. Effects of moose browsing on vegetation and litter of the boreal forest, Isle Royale, Michigan, USA. Ecology 73:2059–2075.

Mermillod-Blondin, F., and R. Rosenberg. 2006. Ecosystem engineering: The impact of bioturbation on biogeochemical processes in marine and freshwater benthic habitats. Aquatic Sciences 68:434–442.

Mulholland, P. J., C. S. Fellows, J. L. Tank, N. B. Grimm, J. R. Webster, S. K. Hamilton, E. Martí, L. Ashkenas, W. B. Bowden, W. K. Dodds, W. H. Mcdowell, M. J. Paul, and B. J. Peterson. 2001. Inter-biome comparison of factors controlling stream metabolism. Freshwater Biology 46:1503–1517.

Munn, M. D., C. P. Konrad, M. P. Miller, and K. Jaeger. 2023. A comparison of spatial and temporal drivers of stream metabolism. Freshwater Biology 68:1751–1764.

Newton, T. J., S. J. Zigler, and B. R. Gray. 2015. Mortality, movement and behaviour of native mussels during a planned water-level drawdown in the Upper Mississippi River. Freshwater Biology 60:1–15.

Nummi, P., M. Vehkaoja, J. Pumpanen, and A. Ojala. 2018. Beavers affect carbon biogeochemistry: Both short-term and long-term processes are involved. Mammal Review 48:298–311.

Olito, C., C. R. White, D. J. Marshall, and D. R. Barneche. 2017. Estimating monotonic rates from biological data using local linear regression. Journal of Experimental Biology 220:759–764.

Pouil, S., A. Hills, and T. J. Mathews. 2021. The effects of food quantity, light, and temperature on clearance rates in freshwater bivalves (Cyrenidae and Unionidae). Hydrobiologia 848:675–689.

Raymond, P. A., J. Hartmann, R. Lauerwald, S. Sobek, C. McDonald, M. Hoover, D. Butman, R. Striegl, E. Mayorga, C. Humborg, P. Kortelainen, H. Dürr, M. Meybeck, P. Ciais, and P. Guth. 2013. Global carbon dioxide emissions from inland waters. Nature 503:355–359.

Reid, A. J., A. K. Carlson, I. F. Creed, E. J. Eliason, P. A. Gell, P. T. J. Johnson, K. A. Kidd, T. J. MacCormack, J. D. Olden, S. J. Ormerod, J. P. Smol, W. W. Taylor, K. Tockner, J. C. Vermaire, D. Dudgeon, and S. J. Cooke. 2019. Emerging threats and persistent conservation challenges for freshwater biodiversity. Biological Reviews 94:849–873.

Ritz, C., F. Baty, J. C. Streibig, and D. Gerhard. 2015. Dose-response analysis using R. PLOS One 10:e0146021.

Roth, F., C. Wild, S. Carvalho, N. Rädecker, C. R. Voolstra, B. Kürten, H. Anlauf, Y. C. El-Khaled, R. Carolan, and B. H. Jones. 2019. An in situ approach for measuring biogeochemical fluxes in structurally complex benthic communities. Methods in Ecology and Evolution 10:712–725.

Schindler, D. E., S. R. Carpenter, J. J. Cole, J. F. Kitchell, and M. L. Pace. 1997. Influence of food web structure on carbon exchange between lakes and the atmosphere. Science 277:248–251.

Schmitz, O. J., and S. J. Leroux. 2020. Food webs and ecosystems: Linking species interactions to the carbon cycle. Annual Review of Ecology, Evolution, and Systematics 51:271–295.

Schmitz, O. J., P. A. Raymond, J. A. Estes, W. A. Kurz, G. W. Holtgrieve, M. E. Ritchie, D. E. Schindler, A. C. Spivak, R. W. Wilson, M. A. Bradford, V. Christensen, L. Deegan, V. Smetacek, M. J. Vanni, and C. C. Wilmers. 2014. Animating the carbon cycle. Ecosystems 17:344–359.

Schmitz, O. J., C. C. Wilmers, S. J. Leroux, C. E. Doughty, T. B. Atwood, M. Galetti, A. B. Davies, and S. J. Goetz. 2018. Animals and the zoogeochemistry of the carbon cycle. Science 362:eaar3213.

Spooner, D. E., and C. C. Vaughn. 2006. Context-dependent effects of freshwater mussels on stream benthic communities. Freshwater Biology 51:1016–1024.

Spooner, D. E., and C. C. Vaughn. 2008. A trait-based approach to species' roles in stream ecosystems: Climate change, community structure, and material cycling. Oecologia 158:307–317.

Steinberg, D. K., and M. R. Landry. 2017. Zooplankton and the ocean carbon cycle. Annual Review of Marine Science 9:413–444.

Steinman, A. D., G. A. Lamberti, P. R. Leavitt, and D. G. Uzarski. 2017. Biomass and pigments of benthic algae. Pages 223–241 *in* F. R. Hauer and G. A. Lamberti (editors). Methods in Stream Ecology. 3rd edition. Academic Press, San Diego, California.

Strayer, D. L., and D. Dudgeon. 2010. Freshwater biodiversity conservation: Recent progress and future challenges. Journal of the North American Benthological Society 29:344–358.

Strickland, M. S., D. Hawlena, A. Reese, M. A. Bradford, and O. J. Schmitz. 2013. Trophic cascade alters ecosystem carbon exchange. Proceedings of the National Academy of Sciences 110:11035–11038.

Taylor, B. W., A. S. Flecker, and R. O. Hall. 2006. Loss of a harvested fish species disrupts carbon flow in a diverse tropical river. Science 313:833–836.

Thomson, A. C. G., S. M. Trevathan-Tackett, D. T. Maher, P. J. Ralph, and P. I. Macreadie. 2019. Bioturbator-stimulated loss of seagrass sediment carbon stocks. Limnology and Oceanography 64:342–356.

Urban, M. 2015. Accelerating extinction risk from climate change. Science 348:571–573.

van Ee, B. C., P. D. Johnson, and C. L. Atkinson. 2022. Thermal sensitivity modulates temporal patterns of ecosystem functioning by freshwater mussels. Freshwater Biology 67:2064–2077.

Vaughn, C. C. 2012. Life history traits and abundance can predict local colonisation and extinction rates of freshwater mussels. Freshwater Biology 57:982–992.

Vaughn, C. C., S. J. Nichols, and D. E. Spooner. 2008. Community and foodweb ecology of freshwater mussels. Journal of the North American Benthological Society 27:409–423.

Wilhm, J. L. 1970. Some aspects of structure and function of benthic macroinvertebrate populations in a spring. American Midland Naturalist 84:20–35.

Wilkens, L. A. 2008. Primary inhibition by light: A unique property of bivalve photoreceptors. American Malacological Bulletin 26:101–109.

Wilmers, C. C., J. A. Estes, M. Edwards, K. L. Laidre, and B. Konar. 2012. Do trophic cascades affect the storage and flux of atmospheric carbon? An analysis of sea otters and kelp forests. Frontiers in Ecology and the Environment 10:409–415.

Wobbrock, J. O., L. Findlater, D. Gergle, and J. J. Higgins. 2011. The aligned rank transform for nonparametric factorial analyses using only ANOVA procedures. Pages 143–146 *in* D. Tan (general chair). CHI ’11: Proceedings of the SIGCHI Conference on Human Factors in Computing Systems. Association for Computing Machinery, Vancouver, British Columbia, Canada.

FIGURE CAPTIONS

Fig. 1. Mussel species included in this study and some of their relevant traits, including mean shell lengths in parentheses (A). Self-contained benthic metabolism chambers used for in situ calculations of ecosystem respiration and gross primary productivity (B), and tracking mussel movement (C). Panel B shows the dissolved O_2 sensor (left), temperature/light logger affixed to a clay tile (center), and recirculating pump (right). Panel C shows the grid system used to track mussel movement. Photographs in panel (A) were taken by Irene Sánchez González.

Fig. 2. Benthic metabolism distribution and scaled coefficient estimates (±SE) for fixed effects included in linear mixed-effects models for ecosystem respiration (ER) (A, B) and gross primary productivity (GPP) (C, D) in benthic metabolism chambers with single-species treatments of 4 mussel species (Ctrl = control, Apli = *Amblema plicata*, Fcer = *Fusconaia cerina*, Lorn = *Lampsilis ornata*, Pkie = *Pustulosa kieneriana*) with contrasting thermal tolerance traits. Treatments with shared lowercase letters above box plots (A, C) cannot be distinguished statistically based on estimated marginal means. Scaled coefficient estimates predict log ER (B) and log GPP (D). In panels A and C, boxes represent the 25th and 75th quartiles, with the central horizontal lines representing the medians. The whiskers extend from the hinge to the value no further than 1.5× above or below the interquartile range. In panels B and D, the vertical dashed line represents a coefficient estimate of 0. Points to the left of this line represent negative standardized coefficient estimates, and points to the right indicate positive coefficient estimates. Temp. = incubation temperature, OM = organic matter, PAR = photosynthetically active radiation.

Fig. 3. Areal chlorophyll *a* concentrations (±SD) from nutrient diffusing substrates in the Sipsey River in western Alabama, USA, in September 2016 at high- and low-mussel density sites (C = control, N = N addition, P = P addition, NP = N + P addition). Treatments with shared lowercase letters cannot be distinguished statistically based on estimated marginal means.

Fig. 4. Horizontal movement distance did not vary with mussel species (A) or thermal tolerance (B). Probability of vertical movement varied with both species (C) and thermal tolerance (D). Mussel burial depth also varied with species (E) and thermal tolerance (F). Treatments with shared lowercase letters cannot be distinguished statistically based on aligned rank transform-C contrasts. Ctrl = control, Apli = *Amblema plicata*, Fcer = *Fusconaia cerina*, Lorn = *Lampsilis ornata*, Pkie = *Pustulosa kieneriana*. In panels E and F, boxes represent the 25th and 75th quartiles, with the central horizontal lines representing the median. The whiskers extend from the hinge to the value no further than 1.5× above or below the interquartile range.

Fig. 5. Scaled coefficient estimates (SE) for the best regression model yielded by a model selection procedure designed to test for potential mussel-driven bioturbation effects on background benthic ecosystem respiration after accounting for mussel organismal respiration. The vertical dashed line represents a coefficient estimate of 0. Points to the left of this line represent negative standardized coefficient estimates, and points to the right indicate positive coefficient estimates. Temp. = mean dark incubation temperature.

Fig. 6. Relative zoogeochemical effect of the 4 mussel-species treatments on benthic CO_2 uptake (Apli = *Amblema plicata*, Fcer = *Fusconaia cerina*, Lorn = *Lampsilis ornata*, Pkie = *Pustulosa kieneriana*). Percentages represent the relative change in mean CO_2 flux between species treatments and the control treatment (control mean CO_2 flux shown as the horizontal dashed line at 0).

Table 1. Type II Wald chi-square test results for fixed effects in linear mixed-effects models of log-transformed benthic ecosystem respiration (log ER) and gross primary productivity (log GPP). OM = organic matter, PAR = photosynthetically active radiation.

Response variable	Fixed effect	χ^2	df	p
Log ER	Biomass	8.5	1	0.004
	Sediment %OM	0.6	1	0.5
	Thermal tolerance	7.7	2	0.02
	Season	16.5	1	<0.0001
	Tolerance × Season	2.2	2	0.3
Log GPP	N excretion	6.3	1	0.01
	P excretion	4.4	1	0.04
	PAR	2.5	1	0.1
	Thermal tolerance	3.6	2	0.2
	Season	7.2	1	0.007
	Tolerance × Season	0.5	2	0.8

Table 2. Results of model selection procedure to identify potential bioturbation effects of mussels on benthic ecosystem respiration. The values under column headers that are named for terms in the model are unstandardized β coefficients. Models shown are those within ΔAICc ≤ 2 of the lowest AICc model. Models are sorted according to adjusted R^2 value. Cells with a dash indicate effects that were not included in a given candidate model.

Intercept	Burial depth	Temperature	Vertical movement	Horizontal movement	Burial depth × temperature	R^2_{adj}	df	AICc	ΔAICc
–24.00	15.300	0.864	–	0.164	–0.632	0.19	6	34.96	1.35
–3.23	0.103	–	–	0.111	–	0.12	5	35.29	1.68
–3.07	0.123	–	–	0.112	–	0.12	4	33.61	0.00
–9.29	0.122	0.257	–	0.125	–	0.11	5	35.59	1.98
–3.18	–	–	–	0.099	–	0.09	4	34.43	0.82
–2.95	0.115	–	0.112	–	–	0.07	4	35.30	1.69
–2.94	–	–	–	0.097	–	0.06	3	33.90	0.29
–2.98	–	–	–	–	–	0.03	3	35.05	1.44
–2.84	–	–	0.097	–	–	0.02	3	35.12	1.51
–2.83	0.099	–	–	–	–	0.02	3	35.13	1.52
–2.75	–	–	–	–	–	0.00	2	34.40	0.79

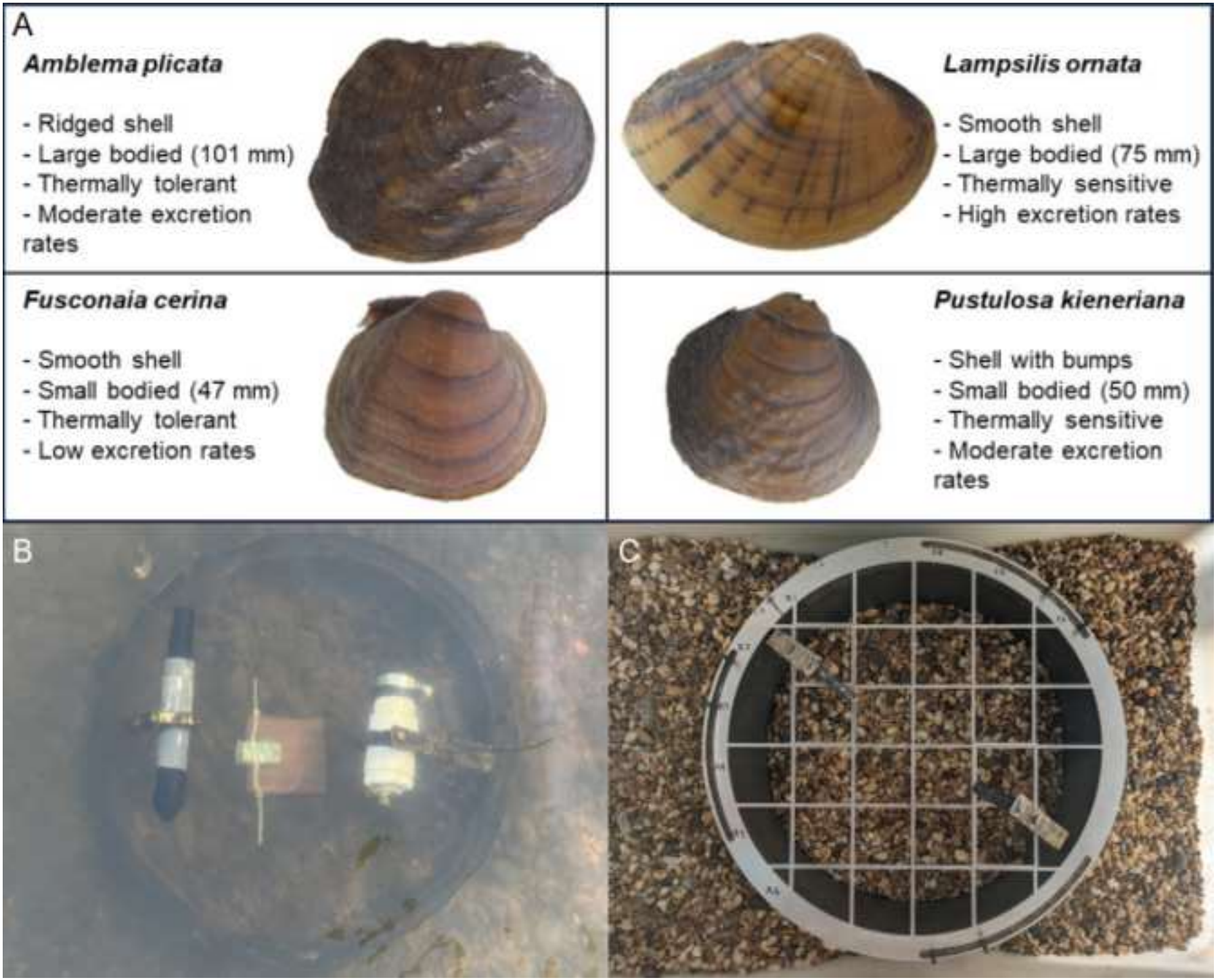

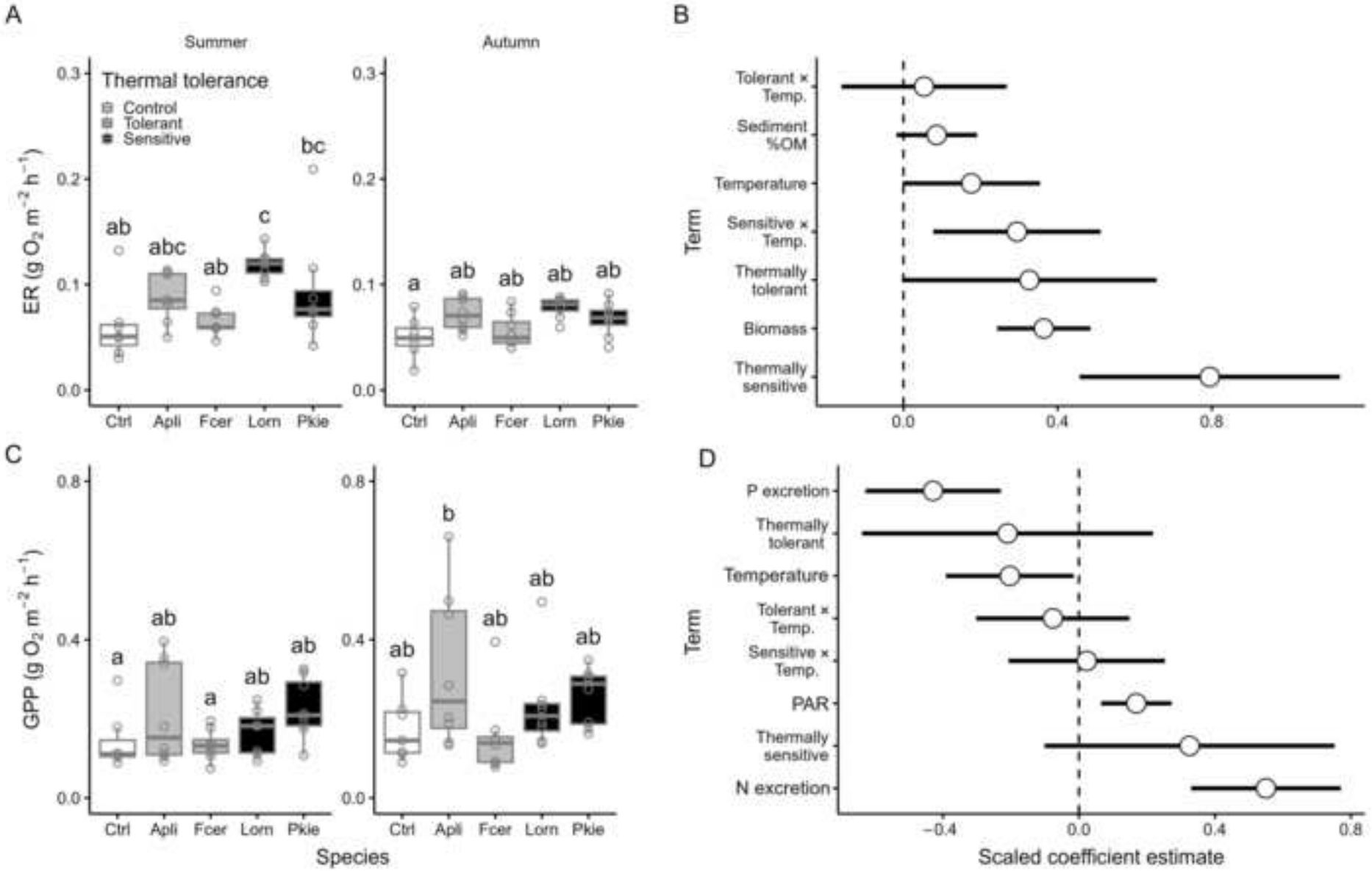

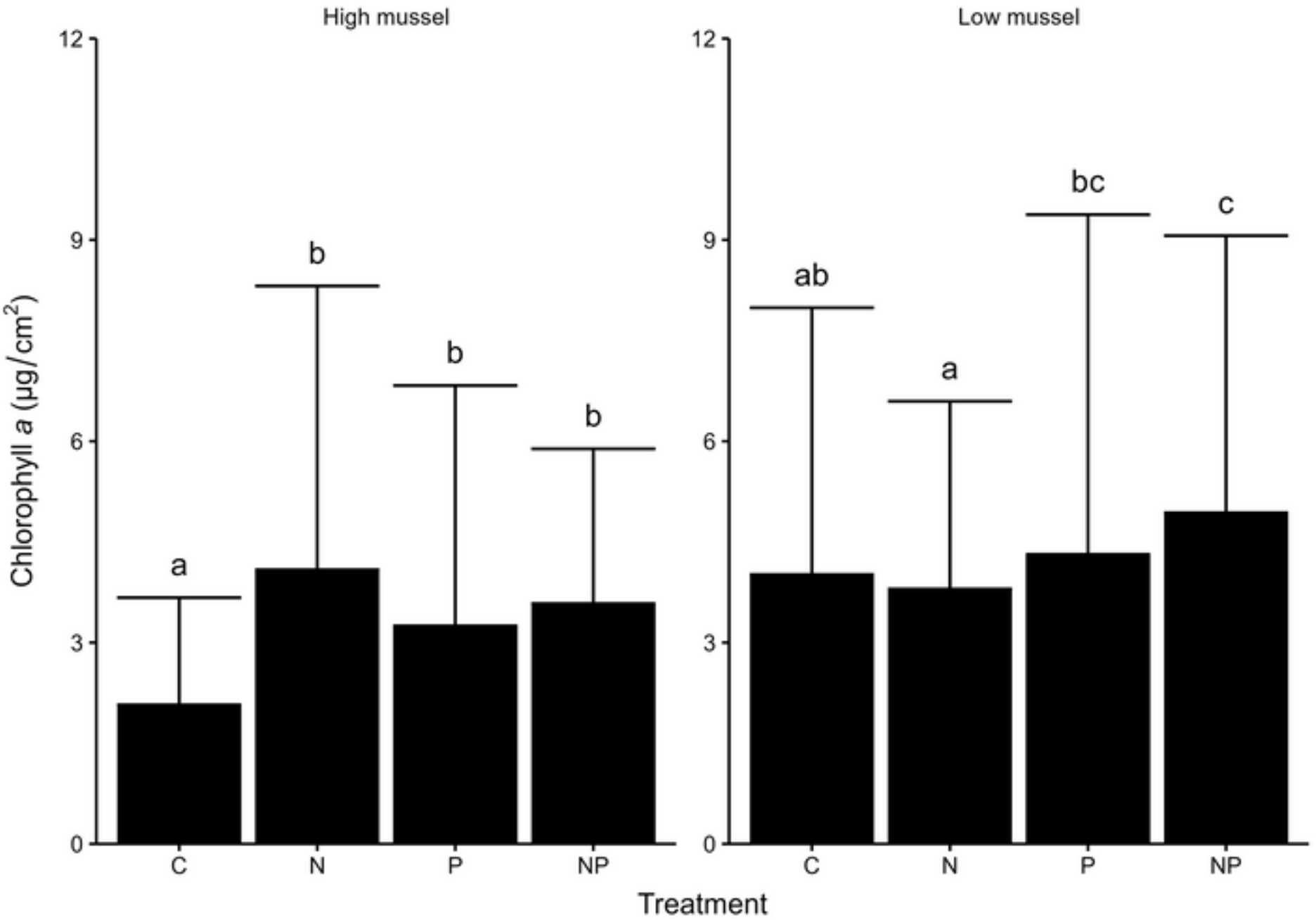

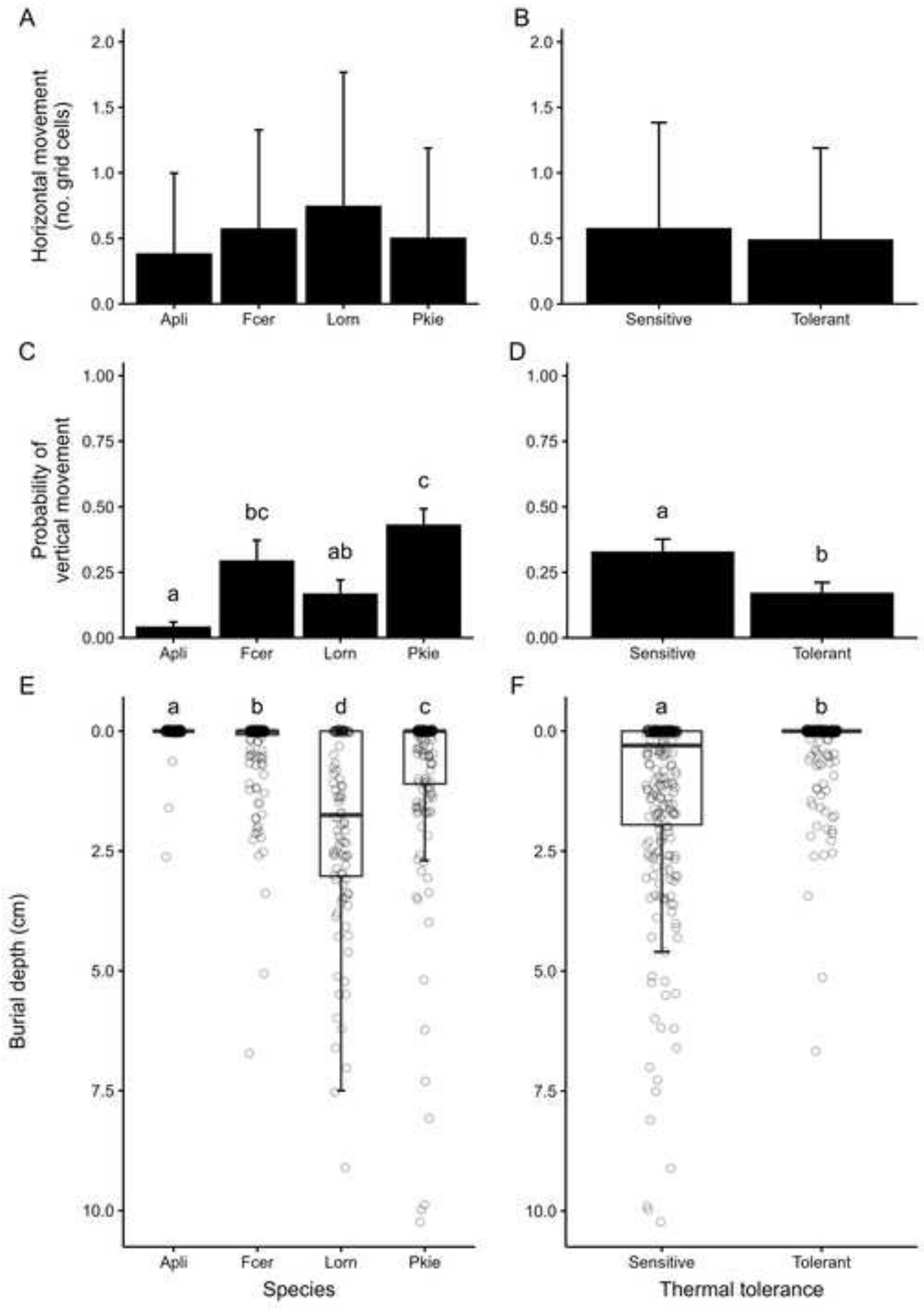

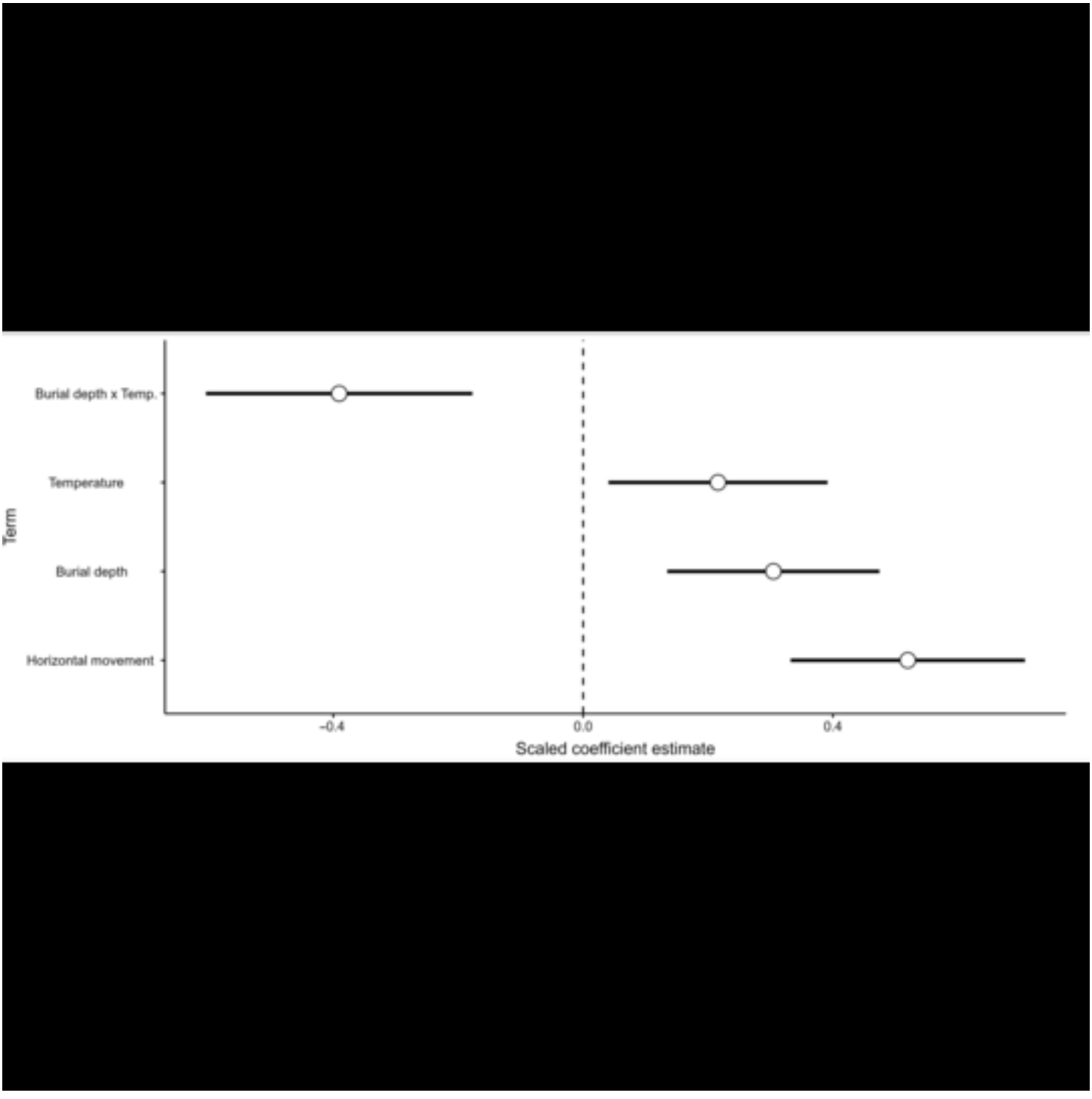

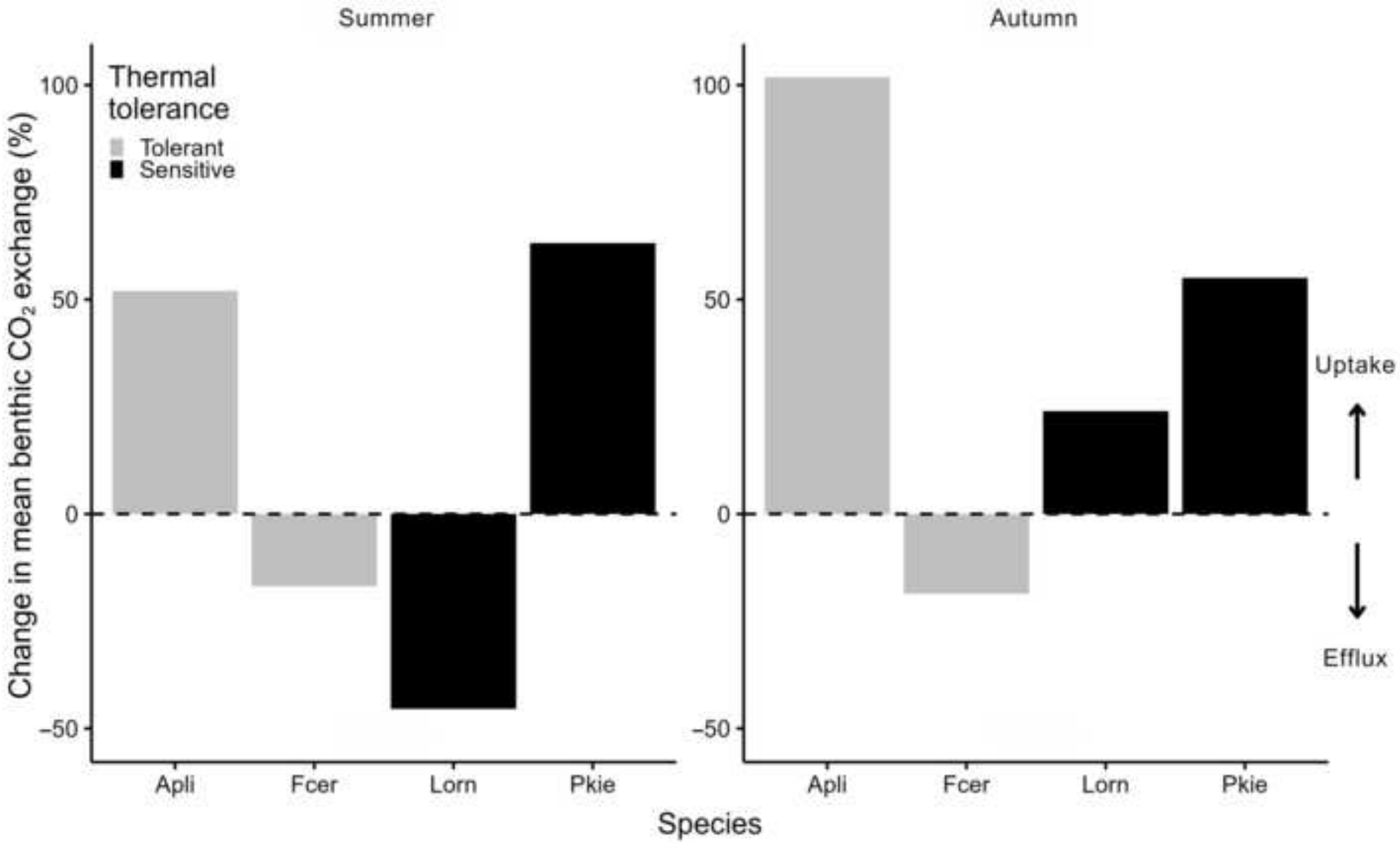

Supplemental material

Zoogeochemical impacts of freshwater mussels on stream metabolism are mediated by their ecophysiological and behavioral traits

Jonathan W. Lopez[1,2], Matthew B. Lodato[1,3], Carla L. Atkinson[1,4]

[1]Department of Biological Sciences, University of Alabama, Tuscaloosa, AL 35487, USA

[2]jwlopez@ua.edu

[3]mlodato@crimson.ua.edu

[4]carla.l.atkinson@ua.edu

Appendix S1

Supplemental methods

Self-contained metabolic incubation chambers. – The self-contained chambers we used were designed to assess benthic metabolic rates in situ. Unlike popular portable chamber designs, which require sediment to be removed from the benthic substratum (Dodds and Brock 1998, Rüegg et al. 2015), our chambers were buried within the substratum, allowing the biological community inside to be in a more natural setting. The chambers were composed of two main parts: a tubular polyvinylchloride (PVC) base (radius = 0.254 m), and a removable hemispheric acrylic dome of equal radius. They were designed to remain buried for weeks to months. We buried the chamber bases in the substratum by excavating the sediment to a depth where the top of the base was nearly flush with the substratum. We prevented backfilling by using a square steel brace, placing each base inside the brace, and refilling the excavated area. Once the bases were embedded in the substratum, we allowed at least two weeks for the benthic communities to return to equilibrium.

To conduct the experiment, the chamber domes were then sequentially affixed to each of the buried bases to create fluid-tight incubation chambers. Each dome had rubber trim around the circumference of the hemisphere to create a seal with the base. The domes also featured two Luer-locking sampling ports that we did not use for the present study and a drain plug, which eases underwater handling. Each base had an acrylic lip that sealed against the bottom of the removable dome. A pair of aluminum holster arms extended upward from each base into the water column. One holster fit a HOBO Dissolved Oxygen Data (DO) Logger (U26-001; Onset Computer Corporation, Bourne, MA, USA) for measuring O_2 fluxes. The other holster fit a recirculating pump constructed from a battery-powered 6 V aquarium pump (flow rate = 1 L min^{-}

^{1}) in a watertight PVC casing. The pump was meant to maintain a constant flow velocity and mix the water column. The domes were submerged and inverted to remove air bubbles, moved into place over the bases, then sealed to the bases with acrylic brackets. Once sealed, we closed the drainplugs and began the incubations.

Excretion. – We measured N (as NH_4^+–N) and P (as soluble reactive phosphorus) excretion rates for one randomly selected mussel from each incubation chamber on 29 September 2023, following the conclusion of the summer incubations. We gently scrubbed mussels with a scour pad to remove biofilms and placed them in plastic containers containing 250–500 mL of filtered stream water (GF/F, 0.7-µm-pore size) depending on the size of the mussel. We also incubated four control containers to account for background nutrient concentrations. We incubated the containers for 1–1.53 h with the chambers placed in shallow stream water to maintain ambient temperatures (23.9°C), then removed the mussels and refiltered the water to isolate soluble excreted nutrients from solid egesta. We retained 15-mL samples of the filtrate and stored them frozen until analysis. We analyzed N (phenol method) and P (colorimetric method) concentrations using a Seal AQ300 discrete analyzer (Seal Analytical, Mequon, WI, USA) (U.S. Environmental Protection Agency 1983). We calculated excretion rates by taking the difference between the nutrient concentrations in each excretion container and the concentrations in the control containers, corrected for incubation time, water volume, and biomass, to get a mass-specific excretion rate for each mussel.

Figure S1. Calibration curve used to estimate photosynthetically active radiation (PAR) from light intensity using a negative exponential model fit. Model equation: $y = 1461\left[1 - e^{(-2.836 \times 10^{-5})x}\right]$.

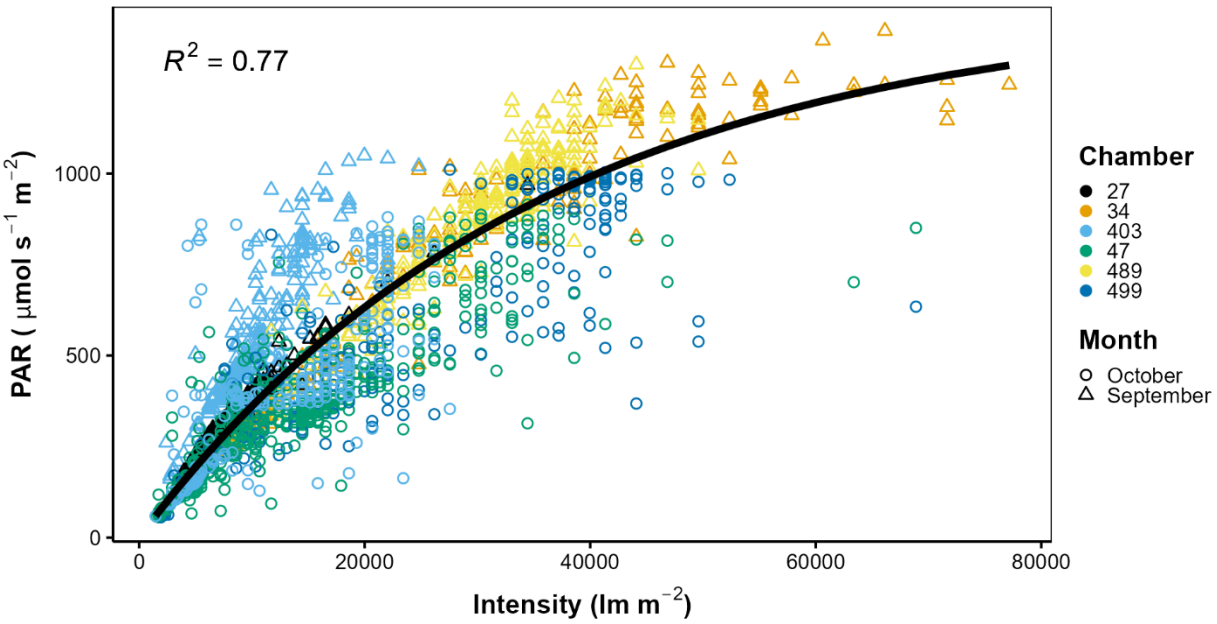

Figure S2. Total nutrient excretion rates for each benthic metabolism chamber in late summer and autumn incubations. Total rates were calculated by scaling mass-specific excretion rates to the amount of mussel biomass in each chamber.

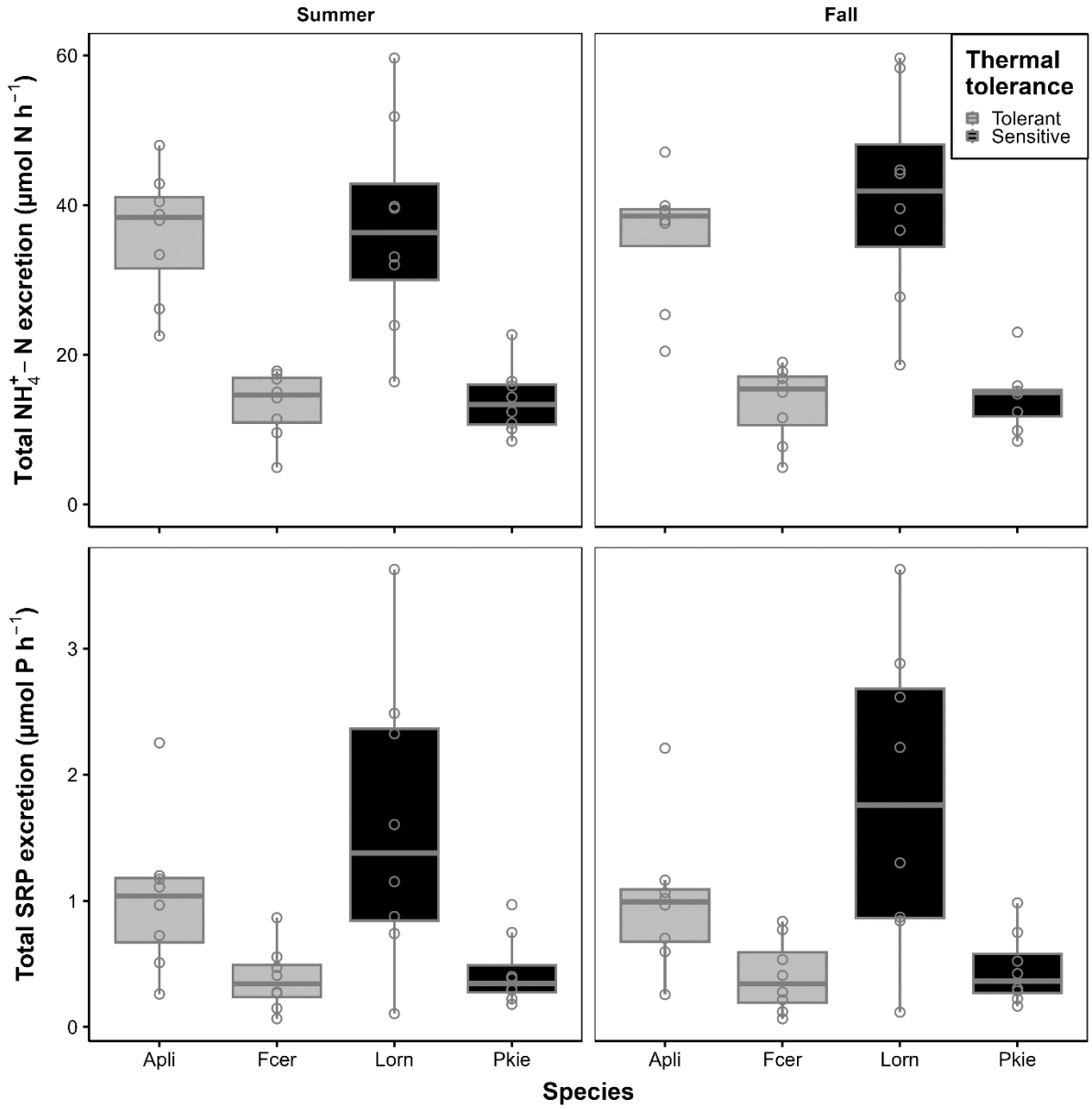

Table S1. Two-way **analysis of variance** table for analysis comparing effects of mussel species and season on ecosystem respiration.

Term	df	Sum of squares	MSE	*F*-value	*p*-value
Species	4	0.02	0.00	7.99	<0.0001
Season	1	0.01	0.01	14.14	<0.0001
Species × Season	4	0.00	0.00	1.13	0.349
Residuals	68	0.04	0.00		

Table S2. Linear mixed-effects model summary table for models of log-transformed benthic ecosystem respiration (marginal $R^2 = 0.41$, conditional $R^2 = 0.57$). OM = organic matter.

Effect	Group	Term	Estimate	SE
Fixed		(Intercept)	-3.569	0.508
Fixed		Biomass	0.011	0.004
Fixed		Sediment %OM	0.179	0.217
Fixed		Thermally tolerant	-0.020	0.602
Fixed		Thermally sensitive	-0.498	0.615
Fixed		Temperature	0.023	0.023
Fixed		Tolerant × Temperature	0.007	0.028
Fixed		Sensitive × Temperature	0.038	0.028
Random	Chamber	SD (Intercept)	0.162	
Random	Residual	SD (Observation)	0.265	

Table S3. Two-way analysis of variance table for analysis comparing effects of mussel species and season on gross primary productivity.

Term	df	Sum of squares	MSE	*F*-value	*p*-value
Species	4	0.17	0.04	4.02	0.006
Season	1	0.05	0.05	4.91	0.030
Species × Season	4	0.02	0.01	0.47	0.758
Residuals	67	0.72	0.01		

Table S4. Linear mixed-effects model summary table for models of log-transformed benthic gross primary productivity (marginal $R^2 = 0.24$, conditional $R^2 = 0.57$). PAR = photosynthetically active radiation.

Effect	Group	Term	Estimate	SE
Fixed		(Intercept)	-1.462	0.703
Fixed		N excretion	0.016	0.007
Fixed		P excretion	-0.255	0.118
Fixed		PAR	0.386	0.237
Fixed		Thermally tolerant	0.165	0.817
Fixed		Thermally sensitive	0.080	0.848
Fixed		Temperature	-0.033	0.031
Fixed		Tolerant × Temperature	-0.012	0.037
Fixed		Sensitive × Temperature	0.004	0.037
Random	Chamber	SD (Intercept)	0.292	
Random	Residual	SD (Observation)	0.337	

Table S5. Two-way analysis of variance table for analysis comparing effects of nutrient addition treatment and mussel presence on benthic algal accrual (as chlorophyll *a*). N = NO_3^-, P = PO_4^{3-}, NP = N + P.

Effect	Group	Term	Estimate	SE
Fixed		(Intercept)	4.423	1.587
Fixed		N	-0.625	0.387
Fixed		P	0.454	0.399
Fixed		NP	1.420	0.402
Fixed		High mussel	-2.178	2.147
Fixed		N × High mussel	2.483	0.524
Fixed		P × High mussel	0.677	0.536
Fixed		NP × High mussel	-0.159	0.536
Random	Site	SD (Intercept)	3.492	
Random	Residual	SD (Observation)	1.791	

Table S6. Analysis of variance table for aligned rank-transformed horizontal mussel movement data. Sums of squares and MSE do not apply for rank-transformed data.

Term	df	*F*-value	*p*-value
Species	3	1	0.401
Error (tag)	131		

Table S7. Analysis of variance table for aligned rank-transformed horizontal mussel movement frequency data. Sums of squares and MSE do not apply for rank-transformed data.

Term	df	*F*-value	*p*-value
Thermal tolerance	3	0.3	0.6
Error (tag)	133		

Table S8. Generalized linear mixed-effects model (binomial distribution, logit link function) summary table for models of variation in mussel vertical movement frequency depending on species (marginal $R^2 = 0.26$, conditional $R^2 = 0.53$). Parameter estimates are relative to a baseline, in this case, the behavior of *Amblema plicata*.

Effect	Group	Term	Estimate	SE
Fixed		(Intercept)	-3.836	0.703
Fixed		*Fusconaia cerina*	2.666	0.726
Fixed		*Lampsilis ornata*	1.583	0.784
Fixed		*Pustulosa kieneriana*	3.477	0.766
Random	Tag	SD (Intercept)	1.360	

Table S9. Generalized linear mixed-effects model (binomial distribution, logit link function) summary table for models of variation in mussel vertical movement frequency depending on thermal tolerance (marginal $R^2 = 0.05$, conditional $R^2 = 0.49$). Parameter estimates are relative to a baseline, in this case, the behavior of thermally sensitive mussels.

Effect	Group	Term	Estimate	SE
Fixed		(Intercept)	-1.144	0.353
Fixed		Thermally tolerant	-1.185	0.462
Random	Tag	SD (Intercept)	1.664	

Table S10. Analysis of variance table for aligned rank-transformed mussel burial depth data. Sums of squares and MSE do not apply for rank-transformed data.

Term	df	*F*-value	*p*-value
Species	3	40.8	<0.0001
Error (tag)	196		

Table S11. Analysis of variance table for aligned rank-transformed mussel burial depth data. Sums of squares and MSE do not apply for rank-transformed data.

Term	df	*F*-value	*p*-value
Thermal tolerance	3	70.9	<0.0001
Error (tag)	198		

Table S12. Analysis of variance table for type II *F* tests of terms explaining background ecosystem respiration.

Term	Sum of squares	df	*F*-value	*p*-value
Burial depth	0.40	1	3.0	0.10
Temperature	0.12	1	0.9	0.36
Horizontal movement	1.03	1	7.7	0.01
Temperature × burial depth	0.45	1	3.4	0.08
Residuals	3.34	25		

Table S13. Linear regression parameter estimates terms explaining background ecosystem respiration (R^2 = 0.19).

Term	Estimate	SE
(Intercept)	-23.965	10.383
Burial depth	15.342	8.313
Temperature	0.864	0.429
Horizontal movement	0.164	0.059
Temperature × Burial depth	-0.632	0.345

Literature cited

Dodds, W. K., and J. Brock. 1998. A portable flow chamber for *in situ* determination of benthic metabolism. Freshwater Biology 39:49–59.

Rüegg, J., J. D. Brant, D. M. Larson, M. T. Trentman, and W. K. Dodds. 2015. A portable, modular, self-contained recirculating chamber to measure benthic processes under controlled water velocity. Freshwater Science 34:831–844.

U.S. Environmental Protection Agency. "Methods for Chemical Analysis of Water and Wastes." Cincinatti, Ohio, USA: Environmental Monitoring and Support Library, 1983.